Forest Ecology and Management 270 (2012) 54–65

Contents lists available at SciVerse ScienceDirect

Forest Ecology and Management

journal homepage: www.elsevier.com/locate/foreco

Estimating leaf area index in intensively managed pine plantations using airborne laser scanner data

Alicia Peduzzi [a,*], Randolph H. Wynne [a], Thomas R. Fox [b], Ross F. Nelson [c], Valerie A. Thomas [d]

[a] Virginia Polytechnic Institute and State University, Department of Forest Resources and Environmental Conservation, 319 Cheatham Hall (Mail Code: 0324), Blacksburg, VA 24061, USA
[b] Virginia Polytechnic Institute and State University, Department of Forest Resources and Environmental Conservation, 228 Cheatham Hall (Mail Code: 0324), Blacksburg, VA 24061, USA
[c] NASA/GSFC, Mail Code 618, Greenbelt, MD 20771, USA
[d] Virginia Polytechnic Institute and State University, Department of Forest Resources and Environmental Conservation, 307A Cheatham Hall (Mail Code: 0324), Blacksburg, VA 24061, USA

ARTICLE INFO

Article history:
Received 11 October 2011
Received in revised form 29 December 2011
Accepted 30 December 2011
Available online 8 February 2012

Keywords:
Loblolly pine
Silviculture
Forest management
Remote sensing
Forest mensuration

ABSTRACT

The objective of this study was to determine whether leaf area index (LAI) can be accurately estimated in intensively managed pine plantations using multiple-return airborne laser scanner (lidar) data. In situ measurements of LAI were made using the LiCor LAI-2000 Plant Canopy Analyzer on 109 plots under a variety of stand conditions (i.e., stand age, nutritional regime, and stem density) in North Carolina and Virginia, USA in late summer, 2008. Distributional metrics were calculated for each plot using small footprint lidar data (average pulse density 5 pulses per square meter; up to four returns per pulse) acquired in the month preceding the field measurements. Distributional metrics were calculated for each plot using all vegetation returns, as well as using ten 1 m deep crown density slices (a new technique introduced in this study), five above and five below the mode of the vegetation returns for each plot. These metrics were used as independent variables in best subsets regressions with LAI (measured in situ) as the dependent variable. The best resulting models had an R^2 ranging from 0.61 (for a 2-variable model) to 0.83 (for a 6-variable model). The laser penetration index (LPI) was an important variable regardless of the number of variables used. Other important variables included the mean intensity value, the mean and 20th percentile of the vegetation returns, and various crown density slice metrics. These results indicate that LAI can be estimated accurately using lidar data in intensively managed pine plantations over a wide variety of stand conditions.

1. Introduction

Stemwood production is influenced by climate, nutrients, and water, but is also determined by the amount of light intercepted and the photosynthetic efficiency of canopies (Vose and Allen, 1988). Canopy structure throughout the vertical and horizontal profiles can be described by biophysical forest parameters such as leaf area and tree height. Leaf area index (LAI) is defined as the total one-sided area of leaf tissue per ground surface area (Watson, 1947). It plays an important role in several key ecosystem processes by the exchange of energy and gases (e.g., CO_2 and water-vapor fluxes) between terrestrial ecosystems and the atmosphere. It is also central to describing rainfall interception. As a result, leaf area varies along with hydrological, biogeochemical, and biophysical processes, either due to natural stand development or forest management practices (e.g., thinning, fertilization, and vegetation control).

Along with leaf biomass, leaf area has a strong relationship with productivity (Cannell, 1989). In loblolly pine (*Pinus taeda* L.), for example, leaf biomass dynamics are dependent on phenology, climatic conditions, site factors and stand density, thus LAI represents a measure of site occupancy that integrates tree size, stand density and site resource supply (Vose and Allen, 1988). Based on these relationships, forest managers have observed crown development and leaf production as responses to fertilization and thinning; such responses are consequently related to carbon accumulation and tree growth (Albaugh et al., 1998; Carlyle, 1998; Martin and Jokela, 2004). Traditional approaches to directly estimate leaf area index, such as using destructive sampling, although very accurate, are labor intensive, time consuming, and costly. The resulting paucity of samples limits their utility for forest management.

The use of remote sensing technologies to monitor, and therefore to improve the management of forest resources at regional

* Corresponding author.
E-mail addresses: apeduzzi@vt.edu (A. Peduzzi), wynne@vt.edu (R.H. Wynne), trfox@vt.edu (T.R. Fox), ross.f.nelson@nasa.gov (R.F. Nelson), thomasv@vt.edu (V.A. Thomas).

0378-1127 Published by Elsevier B.V. Open access under CC BY-NC-ND license.
doi:10.1016/j.foreco.2011.12.048

and global scales has increased exponentially over the last 30 years (Lefsky et al., 2002b; Lu, 2006; Lutz et al., 2008). Previous research has shown that satellite data can be used to estimate LAI accurately in areas where LAI has been empirically related to satellite-measured reflectance values (Curran et al., 1992; Gholz et al., 1997; Jensen and Binford, 2004; Flores et al., 2006). Green vegetation amounts and leaf area index have been associated with spectral reflectance, and frequently with vegetation indices. Nonetheless, researchers have observed that optically-derived vegetation indices reach an asymptote or saturation point when LAI values are on the order of 3–5 (Spanner et al., 1990b; Turner et al., 1999; Birky, 2001; Anderson et al., 2004).

The estimation of LAI using satellite data can be complicated by variation in atmospheric characteristics, the background optical properties (i.e., understory vegetation, senescent leaves, soil, bark and shadows) (Spanner et al., 1990a; Eriksson et al., 2006), and the challenge of accounting for tree architecture (Soudani et al., 2002). A drawback of optical imagery is that it is only appropriate for examining the variation of features on horizontally distributed basis. Newer remote sensing technologies such as discrete return lidar (light detection and ranging), which is physically oriented and generates data points in a three-dimensional cloud, can be suitable to evaluate variation in vertically distributed canopy features. Researchers have employed lidar to estimate forest biophysical parameters, especially in forest inventory applications, such as estimating stand height and volume (Nilsson, 1996; Næsset, 1997a,b; Popescu et al., 2002); forest biomass (Nelson et al., 1997; Lefsky et al., 2002a; Drake et al., 2003; Bortolot and Wynne, 2005; van Aardt et al., 2006); canopy structure (Nelson et al., 1984; Lovell et al., 2003); tree crown diameter (Popescu et al., 2003); stem density (McCombs et al., 2003; Maltamo et al., 2004), species classification (Farid et al., 2006; Ørka et al., 2009) and leaf area index (Morsdorf et al., 2006; Jensen et al., 2008; Zhao and Popescu, 2009). The studies in which lidar data were used to estimate LAI did not find a maximum LAI or saturation problems. However, none of the past studies have used multiple return lidar data to examine the accuracy of lidar-based LAI estimates in stands that have been fertilized at different rates and have different stem densities. The primary objective of this study was to predict LAI accurately across multiple sites of loblolly pine plantations and under a variety of intensive silviculture regimes using laser technology. Traditional approaches, used in previous published work, to extract information from lidar data were followed, as well as the calculation and evaluation of new metrics to better explain variation in LAI.

2. Methods

2.1. Study sites

Five study sites located in North Carolina and Virginia, USA were used for this research. All five sites were established and maintained in support of research studies investigating the role of intensive management in optimizing loblolly pine (*P. taeda* L.) production. These studies were established and/or maintained as a joint effort among the Forest Productivity Cooperative (FPC, 2011), academic institutions, the USDA Forest Service, the Virginia Department of Forestry, and private industry.

The *Nutrient by Stand Density Study* (*NSD*) was installed in 1998 and is located in Buckingham County, Virginia (37°34′59″N, 78°26′49″W) (Fig. 1), at 184 m above sea level. The aim of the study was to investigate the effects of two tree planting spacings and fertilization on tree growth development. It has three different fertilization regimes: low, medium and high, (designed to achieve a site index (SI) at 25 years of 15, 21 and 24 m, respectively), and two different stem densities (897 and 1794 trees per hectare). Fertilizer applications mainly contained nitrogen and phosphorus. Plot size is 676 m^2 (26 m × 26 m) with each block containing 6 plots, for a total of 18 plots. Refer to Carlson et al. (2009) for a more detailed explanation of the treatments.

The second study site was a recently established trial, *RW195501* (*RW19*), which is part of a regionwide study examining the effects of fertilization and thinning in mid-rotation stands. This trial is located in the Piedmont of Virginia in Appomattox County at 37°26′32″N and 78°39′43″W (Fig. 1). A total of 32 plots were installed in a 13 year old stand. The plots vary in size from approximately 400 to 1280 m^2. At the time of the lidar acquisition in summer 2008, only the plots had been established and no additional silvicultural technique had been applied besides the traditional forest operation practices used in the area.

The third study in Virginia, *RW180601* (*RW18*), is also part of a regionwide study designed with the objective of understanding optimal rates and frequencies of nutrient additions for rapid growth in young stands. The trial is located in a Piedmont site of Brunswick County at 36°40′51″N and 77°59′13″W (Fig. 1). A total of 40 plots were installed in 1999 in a 6-year-old planted stand. These plots had complete weed control and five nutrient treatments, as follows: 0, 67, 134, 201, and 269 kg/ha nitrogen (N) applied with phosphorus (0.1 × N), potassium (0.40 × N) and boron (0.005 × N). Nutrient application frequencies were at 1, 2, 4 and 6 year intervals. Thirty plots were thinned in 2008. Plots vary in size from approximately 400 to 470 m^2.

One of the two sites located in North Carolina, is *The Southeast Tree Research and Education Site* (*SETRES*), geographically positioned in the sand hills at 34°54′17″N and 79°29′W (Scotland County) (Fig. 1). This trial was established in 1992 in an 8-year-old plantation. The aim of the study was to quantify the effects of nutrient and water availability on above and below ground productivity and growth efficiency in loblolly pine. Treatments consisted of nutrient additions (nitrogen, phosphorous, potassium, calcium and magnesium), and irrigation. See Albaugh et al. (1998) for complete site and treatment descriptions. Plot size is 900 m^2 (30 m × 30 m), 4 blocks and 4 plots per block, for a total of 16 plots.

The final site in North Carolina, and also the oldest stand measured, is the *Henderson Long Term Site Productivity Study* (*Henderson*) located at 36°26′52″N, 78°28′23″W (Vance County) (Fig. 1). It was established in 1982 with the objective of monitoring the effects of soil management practices on soil structure, organic matter and nutrient contents, and pine growth. Treatments consisted of two levels of biomass harvest, stemwood only or whole tree removals; two site preparation methods, chop and burn, or shear, pile and disk; and vegetation control for the first 5 years or no vegetation control. Plot measurement size is 450 m^2 (15 m × 30 m), and there are 3 blocks, with 8 plots per block, totaling 24 plots in the study. For a detailed description of the treatments and study, see Vitousek and Matson (1985).

2.2. Field data collection and analysis

2.2.1. Inventory data

All studies were measured during the 2008 dormant season. Total tree height (HT) and height to live crown (HLC) were assessed for every tree within the measurement plots using a Haglöf Vertex hypsometer.

2.2.2. Leaf area measured with an optical sensor

Leaf area index data were assessed using the LiCor LAI-2000 Plant Canopy Analyzer on each plot during late summer (September 7–19, 2008) except for the RW19 trial, which was measured in January 2009. Above canopy readings were recorded remotely every 15 s by placing an instrument in an open field adjacent to the stand during the same date and time that measurements were

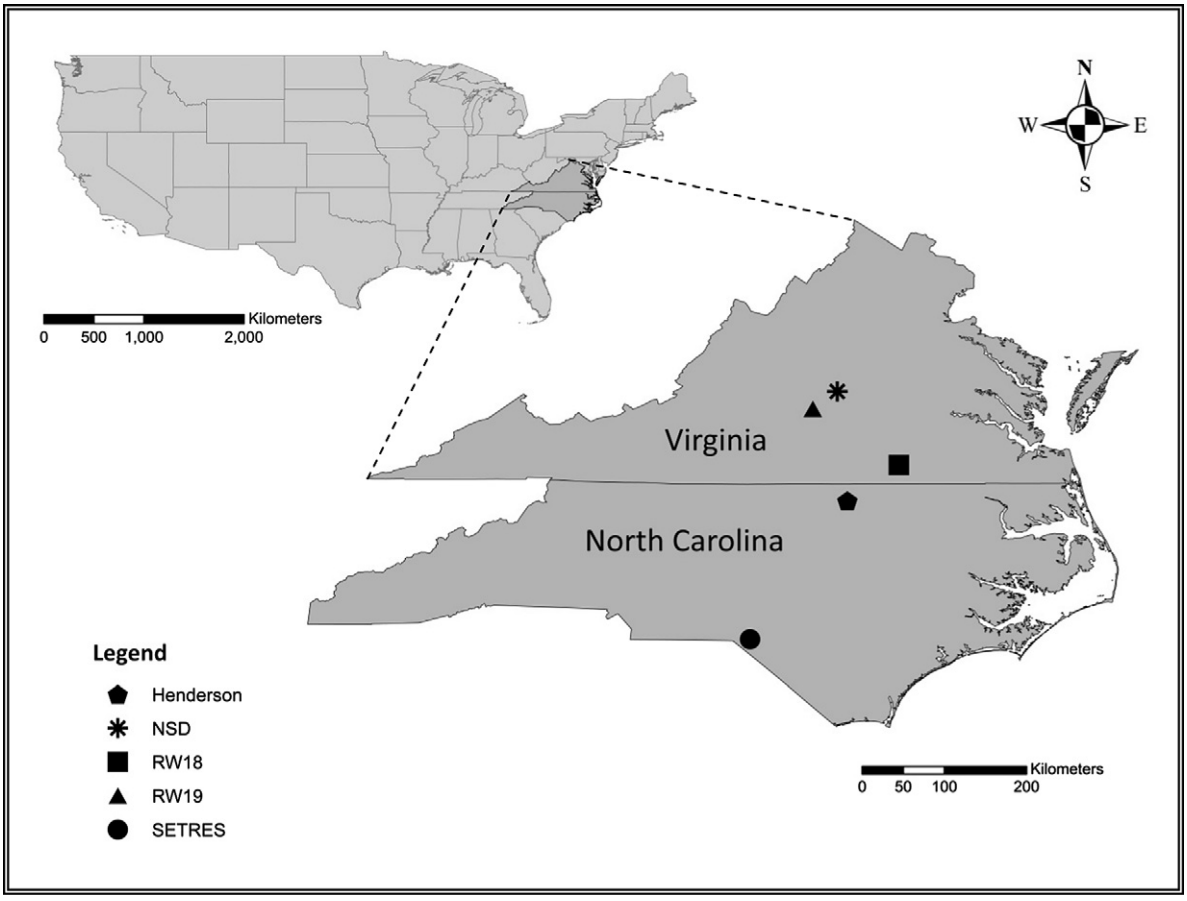

Fig. 1. Geographic representation of the study sites in North Carolina and Virginia, USA.

taken inside the stand. The measurements inside the stand were made holding the instrument at a height of 1 m facing upwards. This same procedure was repeated in every single plot regardless of the presence of understory or mid-story vegetation, such as that found in some plots part of the Henderson study. Due to the instrument's design, measurements were taken under diffuse sky conditions to ensure that the sensor measured only indirect light. Thus, measurements were taken during the dawn and predusk periods, with the above and below instruments facing north, using a 90° view cap. Sampling points were distributed systematically in the plots along a transect perpendicular to the tree-rows. Two transects were used, one close to the plot edge and the other in the middle of the plot. Between 14 and 25 readings were recorded, based on the plot dimensions. The calculation of LAI was accomplished using the FV-2000 software which averaged all the readings per plot. The canopy model used to calculate LAI was Horizontal (LI-COR, 2010); the ring number 5 was masked to reduce the error introduced by the stem and branches of pine trees; the option of skipping records with transmittance >1 was used in order to avoid bad readings that can alter the mean values of LAI per plot. The above and below canopy records were matched by time (Welles and Norman, 1991).

Since RW19 leaf area was measured in early winter (January 2009), a regression model was developed to generate an approximation of the summer 2008 LAI values. The model was based on Licor LAI ground measurements made in summer (August) 2005 and winter (February) 2006 from 17 plots (100 m × 100 m) established in 7- and 10-year old loblolly pine stands. See Peduzzi et al. (2010) for a description of the plots. The resulting equation was $LAI_{summer} = 1.2768(LAI_{winter})$ and had an R^2 of 0.8. Previous research has shown that loblolly pine LAI differences between summer and winter estimates, based on litterfall, are higher than the differences of seasonal LAI estimates using the Licor LAI-2000 (Hebert and Jack, 1998; Dewey et al., 2006), this is probably due to Licor underestimations of LAI (Sampson and Allen, 1995); hence, predicted LAI values from the developed equation were low compared to litter trap estimates (Gresham, 1982; Dalla-Tea and Jokela, 1991) but in agreement with Licor measurements (Sampson et al., 2003). In addition, an unrealistic estimated LAI value (0.12) collected in one of the heavily thinned plots of the RW18 study was deleted from the dataset.

2.2.3. Lidar data

Small footprint lidar data were acquired for all the study areas in late August 2008. The system was an Optech ATLM 3100 with an integrated Applanix DSS 4K × 4K DSS camera. The data have multiple returns with a sampling density of 5 pulses per square meter, with at least 4 returns per pulse. The scan angle was less than 15°. Instrument vertical accuracy over bare ground is 15 cm, and horizontal accuracy is 0.5 m.

Ground returns were already extracted by the lidar provider, and the data were reviewed to determine whether the ground return classification had any flaws. Based on the size of the lidar dataset, these study sites represent a relatively small area, which is an advantage in terms of the computation time necessary to run interpolation models. Therefore, the kriging method was applied to the provided ground returns to generate a digital elevation model (DEM) for the area (Popescu et al., 2002). Next, lidar data points per plot were separated in three classes: "ground returns" (height above the ground, hag = 0 m), "all returns" (hag > 0.2 m),

and "vegetation returns" (hag > 1 m). Vegetation returns were classified using a 1 m threshold because the instrument used to estimate LAI in situ was held at approximately 1 m above the ground. The metrics derived from the ground returns class (Gr) were: frequency (count) of returns and frequency (count) of pulses (Table 1). The metrics derived from the all returns class (All) were: frequency (count), mean height, standard deviation, coefficient of variation, minimum, maximum, percentiles (10, 20, 25, 40, 50, 75, and 90), and frequency (count) of pulses (Magnussen and Boudewyn, 1998; Popescu et al., 2002; Holmgren, 2004). The metrics derived from the vegetation returns class (Veg) were the same described for the all returns class with the addition of the mode. The distribution of intensity values (I) were described using the mean, minimum, maximum, standard deviation, and coefficient of variation. First, second, third and fourth returns were classified as such and divided by the total number of "vegetation returns" (R). The laser penetration index (LPI) (Barilotti et al., 2005), developed taking into account the transmission of the laser beams through the canopy, uses the number of ground returns. It is based on the same principles than the instruments to indirectly measure LAI on the ground (measuring the solar light transmission or reflectance through vegetation). However, the authors advised that this index could vary by forest type and stand structure. LPI was then calculated per plot as the proportion of ground pulses to the total pulses (ground pulses + all pulses). Density metrics (d) were calculated following Næsset (2002), as the proportion of returns found on each of 10 sections equally divided within the range of heights of vegetation returns for each plot. These 10 sections correspond to the 0, 10, 20, ..., 90 quantiles of the return classes per plot. Additionally, another set of metrics, crown density slices (Cd), was calculated using the mode value of vegetation returns. Ten 1-m sections of vegetation returns (5 above and 5 below the mode value, based on the maximum value of crown length observed) were classified and proportion of returns to the total number of returns, mean, standard deviation, and coefficient of variation were calculated (Fig. 2). Frequency of returns (count), calculated from each of the lidar data point classes, were used only to estimate other metrics, such as proportions of returns, but they were not used in the development of the models (Table 1).

The height values obtained from the lidar data collected in RW18 were too high in one portion of the study area, with values several meters higher than the forest stand heights. A threshold, maximum return hag $\geqslant$1 m higher than field-measured tree height per plot was used to eliminate erroneous lidar measurements. After this threshold was applied only 19 plots remained in this study area.

2.2.4. Statistical analysis

A dataset of 109 plots was assembled with all lidar derived metrics and ground truth measurements. Results from the data diagnostic methods applied to the dataset showed normality between the Studentized residuals and the predicted values, and normal order statistics. There was no need to transform the dependent variable, and because the existing outliers were also influential points, they were not deleted from the dataset. Pearson correlation coefficients were used to evaluate relationships among lidar metrics, ground data, and LAI. Multiple regressions were used to fit the dataset. Best subset regression models were examined using the RSQUARE method for best subsets model identification (SAS, 2010). This method generates a set of best models for each number of variables (1, 2, ..., 6, etc.). The criterion to choose the models was a combination of several conditions as follows:

- High coefficient of determination (R^2) value.
- Low residual mean square (RMSE).
- Similarity between the adjusted coefficient of determination $R^2_{adj.}$ and R^2 values. The $R^2_{adj.}$ is a rescaling of R^2 by degrees of freedom, hence involves the ratio of mean squares instead of sum of squares.
- Mallows' C_p statistic values (Hocking, 1976). When the model is correct, the C_p is close to the number of variables in the model.
- Low values from two information criteria, the Akaike (1969) Information Criterion (AIC) and Schwarz (1978) Bayesian Criterion (SBC). The AIC is known for its tendency to select larger subset sizes than the true model; hence the SBC was used for comparison, since it penalizes models with larger number of explanatory variables more heavily than AIC.

The best models chosen per subset size (based on number of variables in the models) were evaluated for collinearity issues. Computational stability diagnostics were then used to check for near-linear dependencies between the explanatory variables. In order to make independent variables orthogonal to the intercept and therefore remove any collinearity that involves the intercept, inde-

Table 1
Explanatory variables derived from lidar. Return hag refers to the return height above the ground. Statistics in subscripts were as follows: frequency (total), mean, mode, standard deviation (stdv), coefficient of variation (cv), minimum (min), maximum (max), and height percentiles (10th, 20th, ..., 90th). The metrics Gr_{total}, All_{total}, Veg_{total}, Gr_{pulses}, All_{pulses}, and Veg_{pulses} were determined for calculation of other metrics (i.e., proportions of returns), but were not used for model development.

Lidar metrics	Symbol
Total number of ground returns	Gr_{total}
All returns (return hag > 0.2 m)	All_{total}, All_{mean}, All_{stdv}, All_{cv}, All_{min}, All_{max}, All_{10th}, ..., All_{90th}
Units are meters for all metrics except for All_{total} *and* All_{cv}	
Vegetation returns (return hag > 1 m)	Veg_{total}, Veg_{mean}, Veg_{mode}, Veg_{stdv}, Veg_{cv}, Veg_{min}, Veg_{max}, Veg_{10th}, ..., Veg_{90th}
Units are meters for all metrics except for Veg_{total} *and* Veg_{cv}	
Pulses (number of lidar pulses per return class)	Gr_{pulses}, All_{pulses}, Veg_{pulses}
Laser penetration index (LPI)	$LPI = Gr_{pulses}/(Gr_{pulses} + All_{pulses})$
Intensity values (returns hag > 1 m)	I_{mean}, I_{min}, I_{max}, I_{stdv}, I_{cv}
Units are watts for all metrics except for I_{cv}	
Proportion of 1st, 2nd, 3rd and 4th returns	R_i = total number of i returns/Veg_{total}
R_i is a proportion of returns	i = 1st, 2nd, 3rd, and 4th
Density	$d_i = [x + (Veg_{max} - Veg_{min})/10]/Veg_{total}$
d_i is a proportion of returns	$x = Veg_{min}, 1, \ldots, 10$
	$i = 1, 2, \ldots, 10$
Crown density slices around Veg_{mode}	Cd_i, $Cd_{i_{mean}}$, $Cd_{i_{stdv}}$, $Cd_{i_{cv}}$
See Fig. 2 for a graphic representation of slices	Cd_i = [number of returns in i/(All_{total} + Gr_{total})]
	(i = +1, +2, +3, +4, +5, 0, −1, −2, −3, −4, and −5)
Units are meters for $Cd_{i_{mean}}$, $Cd_{i_{stdv}}$, and $Cd_{i_{cv}}$	i = +1, ..., + 5 at i meters above Veg_{mode}
	i = 0 at Veg_{mode}
Cdi is a proportion of returns	i = −1, ..., −5 at i meters below Veg_{mode}

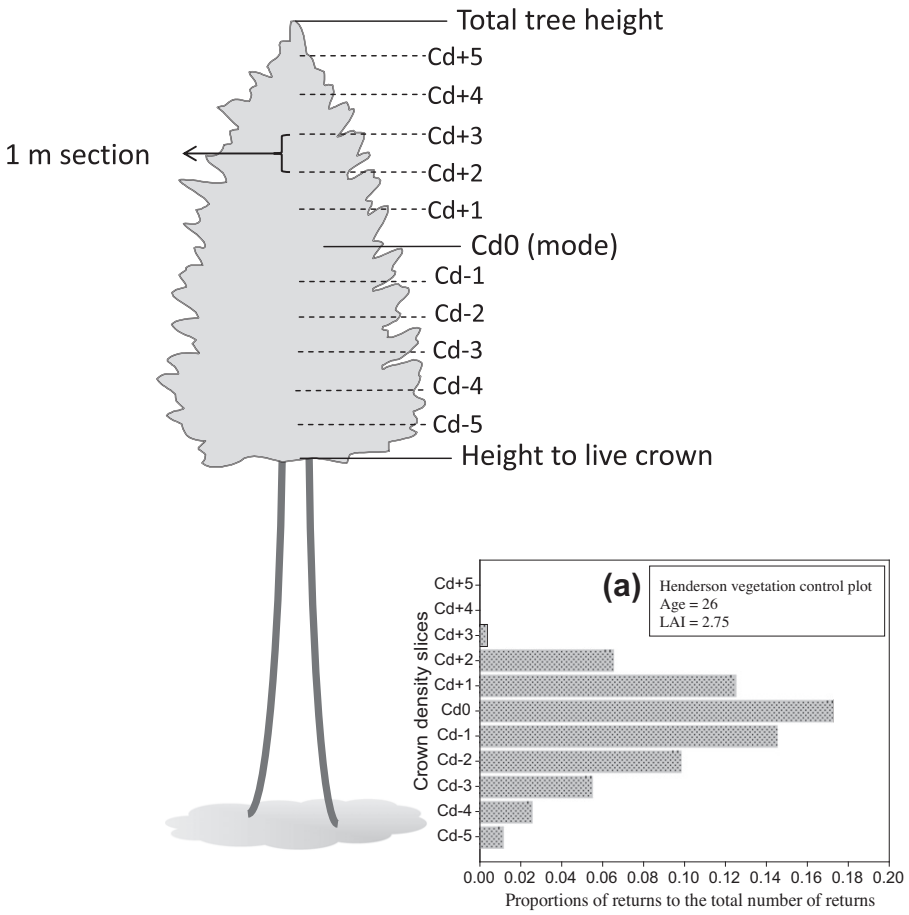

Fig. 2. Graphic description of crown density slices derived from lidar Veg_{mode} value. Mode value per plot was significantly correlated (0.92) with mid-crown height, which was calculated as follows: Tree total height − (crown length/2). Five 1 m sections above and below the mode were defined, and the descriptive statistics (i.e., frequency, mean, standard deviation, and coefficient of variation) from the returns within each section were obtained. See Table 1 for variable names and how they were calculated. (a) Crown density values for a vegetation control plot from the Henderson site.

pendent variables were centered by subtracting their mean values (Marquart, 1980; Belsley, 1984). The variance inflation factor (VIF) quantifies how much the variance of an estimated regression coefficient is inflated, and a threshold of 10 is commonly used, which in the case of higher values, suggests weak ($10 < VIF < 30$) to high ($VIF > 30$) collinearity problems. However, since VIF neither detects multiple near-singularities nor identifies the source of singularities (Rawlings et al., 2001), condition index (CI) was evaluated for all variables within the models. This index is the square root of the ratio of the largest eigenvalue to the corresponding eigenvalue from the matrix. Similar to VIF, the CI indicates weak dependencies when $10 > CI > 30$ to high dependencies when $CI > 30$.

Additional data to test the models were not available, thus cross-validation analysis was performed using the predicted residual sum of the squares (PRESS) statistics (Allen, 1971), which is the sum of squares of the difference between each observation and its prediction when that observation was not used in the prediction equation. The root mean square error from the cross validation analysis (CV-RMSE) was then calculated as the square root of the ratio between the PRESS statistic and the number of observations. The CV-RMSE is an indicator of the predictive power of the model, thus a small CV-RMSE is desirable. The significance level used for all the statistical tests was $\alpha = 0.05$ (p-value < 0.05). This p-value was used to evaluate if the variables included in the model were statistically significant as well. The squared semipartial correlation coefficients (SSCC) were calculated using partial sum of squares to determine the contribution from each variable to the models, while controlling the effects of other independent variables within the model. These coefficients represent the proportion of the variance from the dependent variable associated uniquely with the independent variable.

3. Results

3.1. Summary statistics from ground measurements and lidar metrics

Stand age ranged from 11- to 26-year-old. Forest canopy was closed in all plots, except for the plots in NSD that had the spacing twice as large as that traditionally used in forest operations, and the plots from RW18 that were thinned. Table 2 summarizes the average growth metrics of plots, within the study sites, as treatment and control, and in the case of NSD, these were distinguished by the number of trees per hectare. In RW19 all plots were classified as fertilized, since the stand had been under traditional forest management. Studies in which there were different levels of fertilization were classified together as fertilized, regardless of the rate and frequency of nutrient additions. In RW18, thinning was recently applied to some of the control and fertilized plots, thus the plots at this site were also classified by the number of trees per hectare. Individual tree height ranged from 4.8 to 27.9 m and averaged 15.7 m among all the study areas, the highest standard deviation (>2 m) from the mean of tree height was observed in the SETRES and Henderson studies. Crown length ranged between 0.8 (a damaged tree) and 10.8 m, and averaged 6.9 m. Leaf area in-

dex measured on the ground ranged from 0.45 to 4.91. The lowest values of LAI were observed in the plots from the RW18 study, and they corresponded to the thinned plots which had an average of 16 trees distributed in a 400–470 m^2 plot area. Leaf area index assessment in these plots was expected to be low, not only due to the reduced number of trees, but also due to the difficulty of using an indirect method to measure it. The highest LAI values were observed in the control plots in Henderson. Regardless of the other treatments applied to these plots (harvesting and site preparation), the control plots had consistently higher LAI than the vegetation control plots. In most plots, the presence of competing vegetation (mostly hardwood trees) increased the LAI as much as twice the LAI value from the plots with vegetation control.

Lidar ground returns were lowest (131) at the control plots in Henderson (Table 3). This set of plots can be compared to the vegetation control plots (297) from the same study and to the fertilized plots (223) from RW18, which had comparable tree densities. However, when the number of vegetation returns are taken into account, the proportion of ground pulses relative to the total number of pulses (LPI = 0.08) shows that the canopy in the control plots from Henderson generated more returns (1601) and hence did not penetrate to the ground as much as the other two set of plots. The opposite was observed in the thinned plots from RW18, which had the highest LPI (0.42 and 0.50), and the lowest number of trees per plot, ground penetration was high (461 and 427), and canopy interception low (478 and 670).

Heights of vegetation returns were consistently lower than the tree heights measured on the ground, except for a few returns that were a few centimeters higher than the maximum tree height of the plot. These minor anomalies could be attributable to measurement and estimation errors. Fertilized plots showed higher intensity mean values than control plots; however, as expected, Henderson control plots had higher intensity means than the treated plots, since classification of these plots is not based on nutrient additions but on competing vegetation control.

The vertical profiles (Fig. 3) show graphically the range of heights for the vegetation returns according to their frequency. The mode for each of the sites is highlighted on the profiles; this metric had a Pearson correlation coefficient of 0.92 with the mean mid-crown height of the individual plots (n = 109). The frequency of returns at the Henderson site, and at the RW18 and RW19 sites (Fig. 3) show that there are a number of returns that come from below the canopy, whereas SETRES and NSD frequencies are closer to zero. The latter two sites have been maintained with no understory vegetation. RW18 unthinned plots are also free of understory vegetation, but they represent only 4 of the 19 plots used from this study. The site that showed less frequency of returns was RW18 (Fig. 3); this observation could be due to the fact that most of the 15 plots at this site had been intensively thinned (313–470 TPH) and they are also the smallest plots among all the study sites. SETRES and Henderson have a higher number of trees per hectare than RW19; however the frequency of returns in Fig. 3 was higher in RW19 than in the other two sites. This result could be explained by the number and area of the plots: 32 plots (400–1280 m^2) in RW19, compared to 24 plots (450 m^2) in Henderson, and only 16 plots (900 m^2) in SETRES.

3.2. Variable selection and modeling

Among all the lidar metrics, LPI has the highest correlation with LAI (−0.757) (Table 4). A graphic representation of the LAI and the LPI contrast is shown in Fig. 4, where the high values of LAI are in concordance with the low values of LPI. The crown density slices (1 m section) were calculated with the objective of examining the relationship of the shape of the frequency profiles to LAI. The metrics that contributed to the best models were the proportion of returns at 1 m above the mode (Cd+1) and its standard deviation, the coefficient of variation at 4 m above the mode ($Cd+4_{cv}$), and the proportion of returns at 4 m below the mode (Cd−4). Correlations of these metrics are shown in Table 4. Although the standard deviation at 1 m above the mode ($Cd+1_{stdv}$) was the only one to have a statistically significant correlation with LAI, the other three metrics (Cd+1, $Cd+4_{cv}$, and Cd−4) had a highly significant contribution to the LAI predictive models when used in combination with other variables. The other variables, which were significantly correlated with LAI included Veg_{stdv}, and I_{mean} (Table 4). Also, variables such as the Veg-percentiles, crown density slices, and the rest of the densities, had significant correlations with LAI, but since their correlations were similar to the ones from the variables shown in Table 4, and they were not part of the best models observed, their Pearson coefficients have not been reported. Variables derived from all returns >0.2 m were also significantly correlated with LAI, but not as highly correlated as the variables derived from vegetation returns >1 m. Due to collinearity problems among these metrics, only one set of variables was used at a time in the best subset analysis, and ultimately variables with higher correlations and models with better R^2 were chosen.

All variables from ground measurements showed significant correlations with LAI, that is mean tree height (0.270), mean crown length (−0.343), and number of trees (0.427). However, the best models generated from the best subsets analysis, did not have an increase in R^2 compared to the models using lidar metrics only. Therefore, these models were not reported.

Combinations of the metrics reported in Table 4 for models including 2, 3, 4, 5 and 6 variables are summarized in Table 5. R^2_{adj} values ranged between 0.60 and 0.82 for 2 and 6 variable models, respectively. Despite the collinearity issues that lidar derived metrics can produce in predictive models, all parameters had variance inflation factors (VIF) lower than 6. All variables had a CI lower than 5 (Table 5). The increment in R^2 and R^2_{adj} gained from adding a variable to the model is more noticeable where 2–3 and 3–4 variables were included. The root mean square error (CV-RMSE) and PRESS statistics (from the cross validation analysis) became lower as the number of variables included in the models increased. LPI, which was highly correlated with LAI, was found in all the models, as well as I_{mean} except for the 2-variable model; and as these two variables were added to the models, the Veg_{mean} and Veg_{20th} became common variables also. The variable contributions among the models, in descending order of importance, were LPI, Veg_{mean}, Veg_{20th}, and I_{mean}; except for the 6-variable model were I_{mean} had higher contribution than Veg_{20th}. Crown density metrics were the lesser contributors compared to the rest of the variables, nonetheless these were responsible for increasing the R^2 values from the models. Among all the models reported, the 4-variable model represents the best way to estimate LAI, in terms of maximizing R^2 while minimizing the number of variables. However, predicted LAI values using this model were plotted against the observed LAI from all the plots (Fig. 5) and it was noticeable that one of the plots from RW18 control thinned stands with very low LAI (0.6) was predicted as no LAI (0). Therefore, for comparison purposes, LAI estimations using the 6-variable model were plotted versus the observed LAI values (Fig. 6), in which the same plot was estimated with and LAI of 0.4. Although, the R^2 and R^2_{adj} values are similar between these two models, the 6-variable model predicted low LAI values better (more realistically) than the 4-variable model. Data distribution within the graphs tended to cluster at the center, since this was the range of the observed LAI from most of the sampled plots.

In addition, a modified dataset was used to evaluate the influence that plot size had on the models. As described previously, the area of the plots differed from one site to another. For this modified dataset, all plots were buffered and reduced to the small-

Table 2
Descriptive statistics for tree height, crown length and leaf area index (LAI) at control and treatment plots per study site. Statistics for total were calculated based on plot means. Column annotation: n (number of observations or plots), TPH (trees per hectare), N_{trees} (number of trees per plot), and Stdv (standard deviation).

Study	Stand age	Treatment	n	TPH	N_{trees}	Height (m)				Crown length (m)				LAI			
					(mean)	Mean	Stdv	Range		Mean	Stdv	Range		Mean	Stdv	Range	
NSD	11	Control	3	897	61	11.0	0.9	7.1	12.9	7.2	1.0	6.5	7.6	2.57	0.20	2.38	2.78
			3	1794	125	11.1	0.9	6.5	13.2	5.8	0.9	5.6	6.1	3.72	0.39	3.35	4.13
		Fertilized	6	897	61	11.1	1.0	5.7	13.3	7.3	1.1	6.7	7.9	3.21	0.48	2.51	3.97
			6	1794	123	11.2	0.9	6.7	14.6	5.9	1.0	5.7	6.2	3.50	0.49	2.84	4.03
RW19	13	Fertilized	32	1176	94	13.1	1.3	5.0	18.8	7.3	1.2	6.5	8.0	2.56	0.27	1.93	3.05
RW18	16	Control and thinned	2	(346–395)	16	16.7	0.7	15.5	18.0	7.7	1.0	5.7	10.8	0.79	0.30	0.57	1.00
		Fertilized unthinned	4	1678	60	16.9	1.8	10.5	20.6	6.3	1.6	0.8	10.7	3.90	0.78	2.93	4.85
		Fertilized and thinned	13	(313–470)	16	17.0	0.8	13.8	19.4	7.6	1.0	4.9	10.7	0.96	0.30	0.45	1.52
SETRES	24	Control	4	1665	100	12.9	2.1	4.8	17.8	6.2	1.6	5.7	6.6	2.09	0.38	1.55	2.40
		Fertilized, irrigated or both	12	1665	95	16.6	2.5	6.0	22.1	6.9	1.7	6.1	7.9	2.66	0.41	1.87	3.27
Henderson	26	Control	12	1665	51	21.1	2.4	13.4	27.9	6.3	1.8	5.6	8.2	4.47	0.31	3.84	4.91
		Vegetation control	12	1665	63	21.9	2.2	14.0	26.9	6.2	1.7	5.0	7.1	3.07	0.83	2.08	4.69
Total			109	–	73	15.7	3.7	4.8	27.9	6.9	0.8	0.8	10.8	2.77	1.06	0.45	4.91

est area plots (between 400 and 450 m^2), and lidar metrics for this new set of plots were then calculated. Despite the expectation that the results using similar plot sizes could improve, the models derived using same plot size consistently showed lower R^2 values than those generated using different plot size. Nonetheless, the combination of variables within the models was very similar. This result was supported by the absence of correlation between LAI and plot area ($r = -0.010$).

4. Discussion

Good correlations of certain lidar metrics with LAI were expected. Laser penetration index is physically related to the level of canopy development; the closer and denser the vegetation, the less the laser pulses penetrate to reach the ground. This index has been used in previous research to predict LAI, and reported models were able to explain 80% or more of the variation of leaf area in natural forest ecosystems (Barilotti et al., 2005; Kwak et al., 2007). Vegetation return percentiles, and canopy densities have also correlated well with other stand attributes, including tree height, diameter, and volume (Magnussen and Boudewyn, 1998; Næsset, 2002; Popescu et al., 2002; Holmgren, 2004). Recurrent variables in the models, besides LPI, were:

(1) The average intensity of the returns (I_{mean}), which as a measure of the return signal strength, depends, among other things, on the reflectance and reflectivity of the target. This metric is therefore closely related to the amount of vegetation (leaves and branches) when a forest is such target. Previous research has used metrics calculated from intensity values to estimate forest biomass (van Aardt et al., 2006); however, since the intensity values from lidar sensors are frequently not calibrated, researchers have advised to using them with caution (Bater et al., 2011). Fortunately, the dataset used in this research encompasses large variability in many aspects. Lidar data acquisition dates were not the same for most sites, the terrain relief ranged from flat to hilly, and the forest stands varied in age, stem density and fertilization rates. Therefore, the intensity metrics used for developing the models inherently possessed a large amount of variation.
(2) The average height from the vegetation returns (hag > 1 m) and the Veg_{20th} percentile. These two metrics are lidar return height values, hence they are descriptors of the canopy density and height of the forest stands. The mean values from the lidar returns are related to the distribution of return heights across the stand vertical profiles, and such heights will therefore relate to the target heights (on the

Table 3
Means of lidar returns per plot at each study site. Minimum values for vegetation returns heights above ground were set at 1 m. Intensity minimum value was 1 for all plots (n = 109). Column annotation: n (number of observations or plots), Gr_{total} (total number of ground returns), Veg_{total} (total number of all returns), Stdv (standard deviation), Max (maximum value), and LPI (Laser Penetration Index).

Study	Treatment	n	N_{trees} (mean)	Gr_{total} (mean)	Veg_{total} (mean)	Veg return heights (m)			Intensity (W)			LPI
						Mean	Stdv	Max	Mean	Stdv	Max	
NSD	Control	3	61	592	1286	6.9	1.7	11.5	33.5	14.1	93	0.32
		3	125	719	1965	7.8	1.5	12.1	36.7	13.9	75	0.28
	Fertilized	6	61	589	1912	7.3	1.7	12.1	38.9	14.9	91	0.24
		6	123	660	2218	8.0	1.5	12.1	40.8	14.7	80	0.23
RW19	Fertilized	32	94	1042	2201	9.2	2.1	15.2	36.8	16.0	115	0.30
RW18	Control and thinned	2	16	461	478	12.6	1.9	16.7	28.9	14.5	66	0.50
	Fertilized unthinned	4	60	223	1031	12.5	3.7	18.6	34.5	13.2	71	0.18
	Fertilized and thinned	13	16	427	670	11.9	3.5	19.4	31.4	15.2	87	0.42
SETRES	Control	4	100	814	2806	10.4	2.2	18.1	28.9	13.3	69	0.23
	Fertilized, irrigated or both	12	95	757	2456	14.0	2.7	21.2	34.1	14.6	80	0.24
Henderson	Control	12	63	131	1601	15.2	5.0	24.7	32.0	19.4	103	0.08
	Vegetation control	12	51	297	1395	17.1	5.6	25.7	30.4	15.8	105	0.18

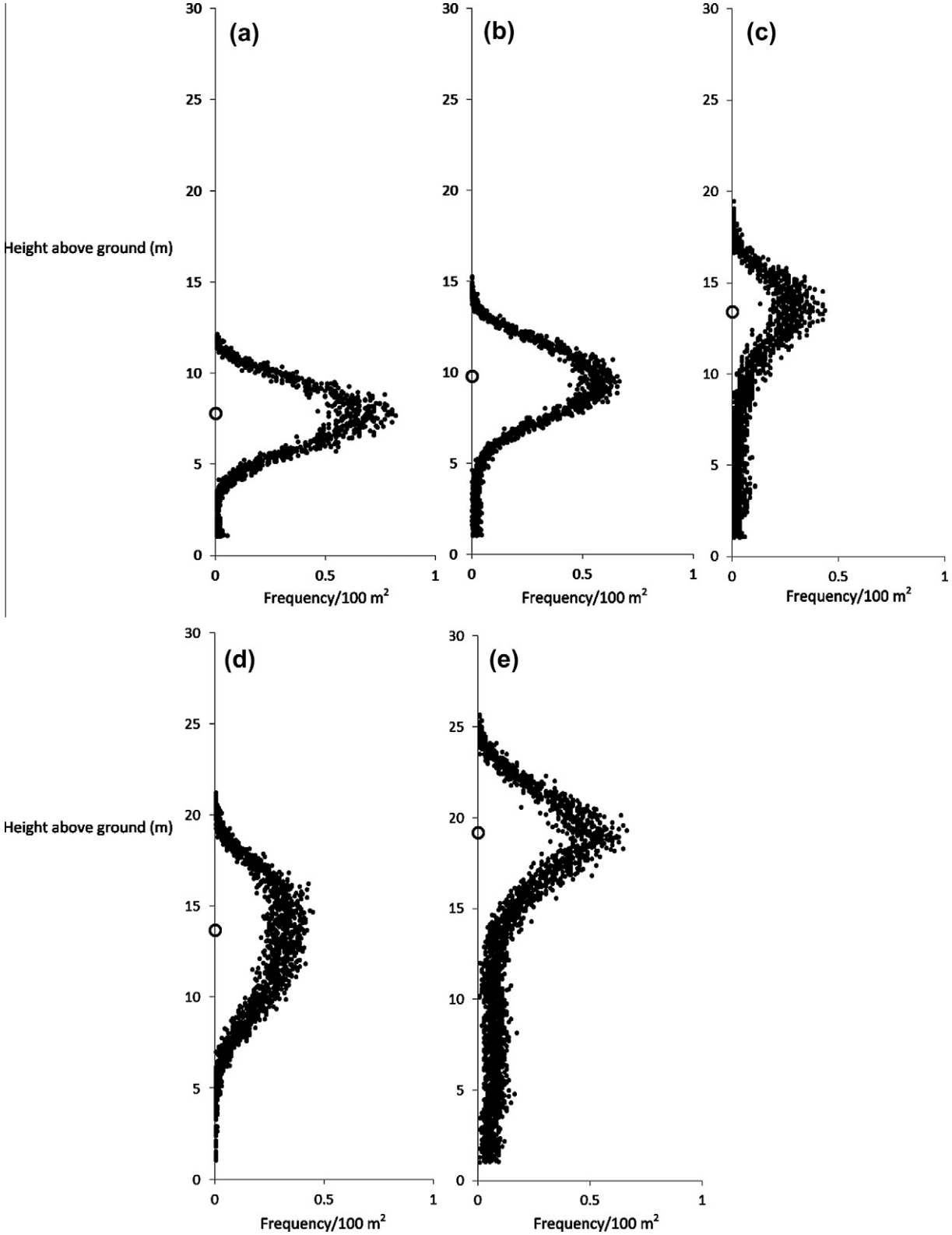

Fig. 3. Vertical profiles for lidar vegetation returns (hag > 1 m) in each study site. The mode for the vegetation returns is circled on the *y* axis. Study sites are: (a) NSD, (b) RW19, (c) RW18, (d) SETRES, and (e) Henderson.

ground). The more targets (i.e., branches, leaves, etc.) the laser would encounter within a range of heights, the more returns will be obtained from that section of the stand. Thus, the mean value from all the vegetation returns will be influenced by the heights from where most of the returns were acquired. Similarly, the percentile values, in this case the 20th, meaning that 80% of the return heights are above that height; can refer to the density of such targets on the ground.

(3) The standard deviation of the returns found between 1 and 2 m above the mode of the height values of vegetation returns ($Cd+1_{stdv}$). This variable had a negative correlation

Table 4
Pearson correlation coefficients for the independent variables used to predict leaf area index (LAI) (n = 109). For a description of the variable names refer to Table 1. LAI was measured on the ground. Bold values were significant at α = 0.05.

	LAI	LPI	Veg_{mean}	Veg_{stdv}	Veg_{20th}	I_{mean}	Cd+1	$Cd+1_{stdv}$	$Cd+4_{cv}$	Cd−4
LAI	1	**−0.757**	0.187	**0.397**	−0.046	**0.271**	0.086	**−0.328**	−0.029	0.101
LPI		1	−0.045	**−0.271**	0.060	**−0.183**	**−0.254**	**0.239**	**−0.213**	−0.185
Veg_{mean}			1	**0.693**	**0.873**	**−0.436**	0.153	−0.004	**−0.453**	**0.391**
Veg_{stdv}				1	**0.366**	**−0.491**	0.024	0.016	**−0.249**	**0.227**
Veg_{20th}					1	**−0.271**	**0.250**	**0.045**	−0.450	**0.298**
I_{mean}						1	0.172	−0.075	0.086	−0.179
Cd+1							1	0.002	**0.304**	**−0.326**
$Cd+1_{stdv}$								1	0.135	0.125
$Cd+4_{cv}$									1	−0.093
Cd−4										1

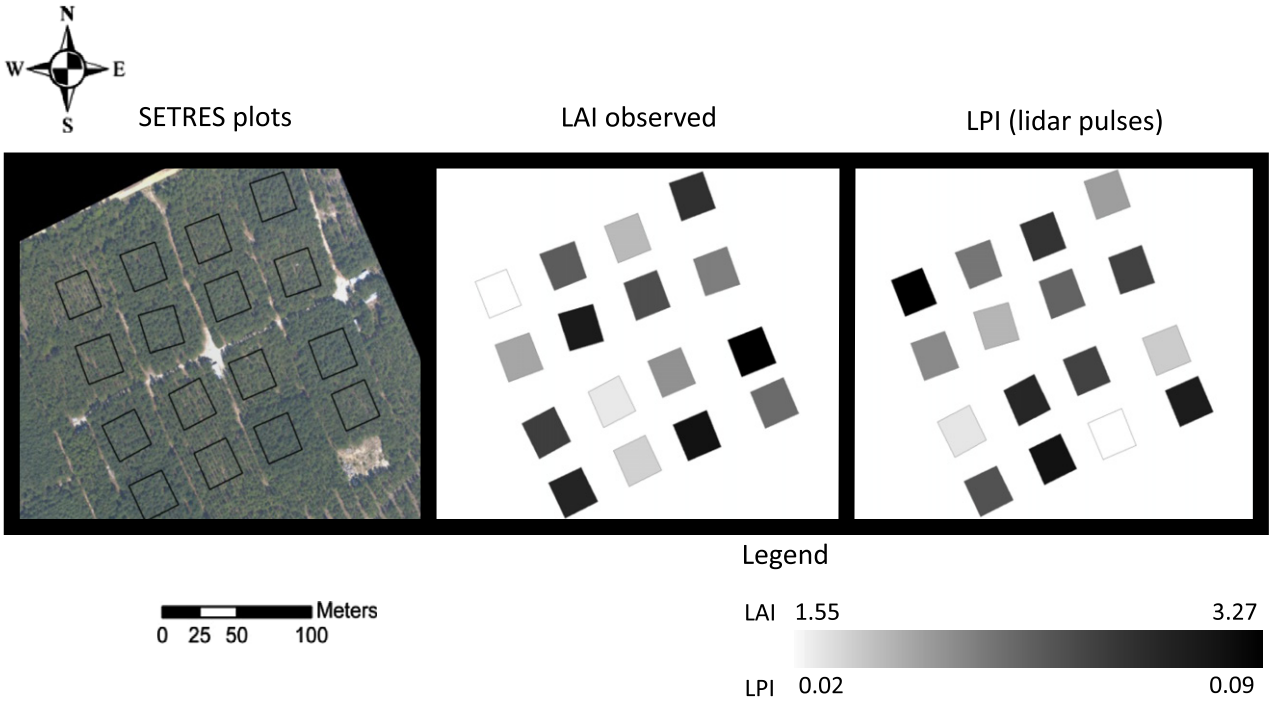

Fig. 4. Graphic representation of LAI and LPI mean values for a subset of plots at the SETRES study site. LAI and LPI have a negative correlation (−0.76), hence when LAI is high (dark) the LPI should be low (light). Aerial photography was taken at the same time that lidar data were acquired (Summer 2008).

with LAI, meaning that the higher the LAI, the less the dispersion observed from the mean of the height values. This section is located above the mode, within the top part of the tree crowns, which in closed canopy stands such as these is likely to be where most of the foliage would be located.

Despite the fact that ground-based variables (number of trees, mean tree height, and crown length) showed significant correlations with LAI, these were not strong enough to increase the performance of lidar metrics when added to the models.

Previously developed leaf area predictive models (that used discrete lidar data, first and last returns) were reported to explain between 40% and 89% of the variance. Interestingly enough, the tendency observed is that relationships (between LAI and lidar metrics) favor the sampling of mixed species forests more than pure coniferous stands. For example, Riaño et al. (2004) measured forests in Spain and reported $R^2 > 0.8$ for deciduous species and $R^2 < 0.4$ for pines. Other researchers modeling pure pine stands reported an R^2 of 0.69 in Sweden (Morsdorf et al., 2006), and an R^2 of 0.70 in the U.S. (Jensen et al., 2008); but the results from mixed species stands have R^2 values of 0.89 (Barilotti et al., 2005), 0.80 (adjusted R^2) (Sasaki et al., 2008), and 0.84 (Zhao and Popescu, 2009). Using loblolly pine plantations only, Roberts et al. (2005) developed a model that explained 69% of the variation.

Based on these previous results, the models obtained performed close to the best models reported in the literature, since they explained up to 83% of the variation. Specially, considering that the stands sampled in the current study were not only pure coniferous stands, but also of uniform age within each site, and growing under intensive management (at different fertilization rates, tree spacing, and little or no understory vegetation). The use of multiple return data might have made the characterization of such variation across the study sites feasible, since many of the variables included in the model were based on the number of returns, instead of using the number of pulses.

A group of models explaining between 61% and 83% of the LAI variation was reported. The reason for this range is the number of variables in each model. Although the most parsimonious model is generally considered best, this applies to cases when the stability of the model can be compromised or when the estimation of an additional variable impact on the research or operation costs, which is usually the case in biological sciences (Rawlings et al.,

Table 5
Best predictive models of LAI using lidar metrics only, $n = 109$. The statistics R^2_{adj}, CV-RMSE, SSCC, VIF, and CI are the adjusted coefficient of determination, the RMSE from the cross validation analysis, the squared semipartial correlation coefficient from partial sum of squares, the variance inflation factor and the condition index, respectively. Since all the explanatory variables were centered, the intercept parameter for all models is 2.767. All variables in the models were highly significant at a p-value <0.0001, except for $Cd+1_{stdv}$ with a p-value <0.01 (in the 5-variable model), and $Cd+4_{cv}$ with a p-value <0.005 (in the 2-variable model). For a description of the variable names refer to Table 1.

Variable No.	R^2	R^2_{adj}	RMSE	CV-RMSE	Variable	Coefficient	SSCC	VIF	CI
2	0.61	0.60	0.67	0.67	LPI	−7.518	0.61	1.05	1.10
					$Cd+4_{cv}$	−0.237	0.04	1.05	1.24
3	0.71	0.70	0.58	0.59	Veg_{stdv}	0.318	0.11	1.60	1.14
					LPI	−5.393	0.26	1.26	1.23
					I_{mean}	0.099	0.09	1.54	2.07
4	0.79	0.779	0.50	0.51	Veg_{mean}	0.330	0.19	5.68	1.40
					Veg_{20th}	−0.268	0.14	4.86	1.45
					LPI	−5.522	0.30	1.14	1.72
					I_{mean}	0.106	0.11	1.44	4.67
5	0.80	0.791	0.48	0.50	Veg_{mean}	0.324	0.19	5.70	1.29
					Veg_{20th}	−0.262	0.13	4.89	1.45
					LPI	−5.275	0.26	1.19	1.60
					I_{mean}	0.104	0.11	1.45	1.75
					$Cd+1_{stdv}$	−13.046	0.01	1.07	4.68
6	0.83	0.82	0.45	0.46	Veg_{mean}	0.345	0.20	5.93	1.27
					Veg_{20th}	−0.236	0.10	5.26	1.42
					LPI	−6.475	0.34	1.38	1.52
					I_{mean}	0.113	0.12	1.47	1.84
					Cd+1	−10.772	0.03	1.64	2.68
					Cd−4	−18.581	0.04	1.64	4.98

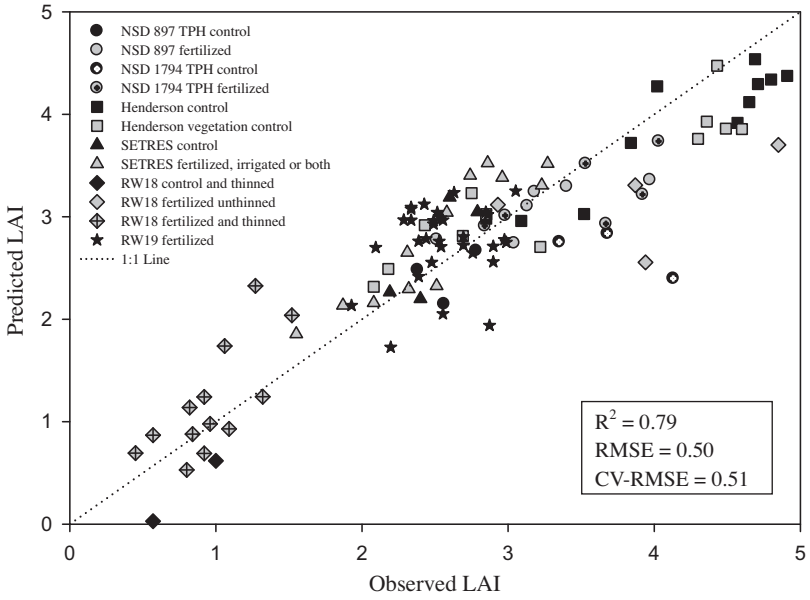

Fig. 5. Relationship between estimated LAI and measured LAI using the 4-variable model with lidar metrics only ($n = 109$). Plots were classified first by stem density, and then by control and treatment. Model (refer to Table 1 for variable names): LAI = 2.767 + 0.330 (Veg_{mean}) − 0.268 (Veg_{20th}) − 5.522 (LPI) + 0.106 (I_{mean}).

2001). Adding a lidar metric to the model will not increase the cost in a significant matter, since the highest cost is the acquisition of the lidar data itself. It will only add computational time, therefore a 6-variable model (with stable regression estimates) for predicting LAI can only increase the accuracy of the predictions. The decision of which model should be used will depend on a forest manager's needs. If a good approximation of the estimates and relative variation of LAI values is sufficient, the 2-variable model will be appropriate, but if higher accuracy is wanted, a 6-variable model will be the best choice.

LAI is a useful index for intensive plantation management because it provides an estimate of the amount of light captured by the stand and is thus a proxy variable that defines the stand's current growing conditions. For instance, LAI allows foresters to identify stands that are in need of fertilization (e.g., when LAI is low) or thinning (e.g., when LAI is high), in order to improve tree growth and maximize returns. The 6-variable model, with an RMSE for prediction (CV-RMSE) of 0.46, provides a precise tool for this type of management, in which decisions are usually made based on LAI thresholds. In this case, an error of this magnitude in estimating LAI for forest management purposes is not as important as the consistency of the estimated values across stands under different conditions (the ability to use the same model across different stand ages, fertilization regimes, vegetation controls, etc.). For forest managers, the advantage of having a model that estimates LAI using remotely sensed data resides in the accuracy and

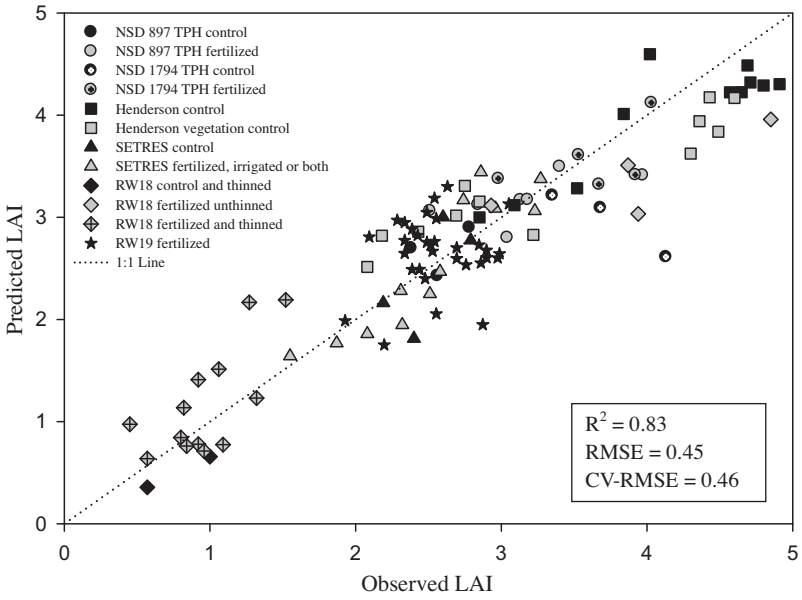

Fig. 6. Relationship between estimated LAI and measured LAI using the 6-variable model with lidar metrics only ($n = 109$). Plots were first separated by stem density, and then by control and treatment. Model (refer to Table 1 for variable names): LAI = 2.767 + 0.345 (Veg_{mean}) − 0.236 (Veg_{20th}) − 6.475 (LPI) + 0.113 (I_{mean}) − 10.772 (Cd+1) − 18.581 (Cd−4).

robustness of such models. Although satellite-derived LAI estimates rely on models with R^2 values similar to those of the lidar model developed in this research (Flores et al., 2006), such estimates have not been consistent, mainly due to issues associated with sensor saturation, atmospheric conditions, and the inability to account for the vertical structure of the stand (Peduzzi et al., 2010). Lidar data are not without acquisition issues; in the past, there have been concerns about the consistency of metrics derived from lidar returns given variations in lidar sensor configurations, flight characteristics, atmospheric conditions, topography, and target objects (Bater et al., 2011). In view of creating a robust model, this research has taken into account much of the variation associated with these issues. For all sites, the sensor configuration was similar; however, the acquisition date and time did not coincide for most of them, topography differed, and, given the different stand ages, stem densities and fertilization regimes included in the dataset, target objects also varied.

5. Conclusion

Laser technology has been successfully used in the past to estimate forest height, volume and biomass to the stand and plot levels. Lately, attempts to estimate leaf area index have broadened the potential of this tool. The results from this research complement these efforts. A robust model with a unique set of variables was developed that explained 83% of the variation of LAI in loblolly pine plantations. The model was constructed from and tested through cross validation on multiple research studies across a wide range of site conditions and silvicultural regimes, giving foresters managing for different purposes (i.e., sawtimber, pulp, etc.) the opportunity to use it as a robust application in decision making.

Acknowledgments

This research was possible thanks to the support from the Forest Productivity Cooperative, and the help in field data collection provided by Rupesh Shrestha, Jessica Walker, Jose Zerpa, Nilam Kayastha, Asim Banskota, Dan Evans, Omar Carrero, Lee Allen, and the personnel from the Virginia Department of Forestry.

References

Akaike, H., 1969. Fitting autoregressive models for prediction. Ann. Inst. Stat. Math. 21, 243–247.
Albaugh, T.J., Allen, H.L., Dougherty, P.M., Kress, L.W., King, J.S., 1998. Leaf area and above- and belowground growth responses of loblolly pine to nutrient and water additions. For. Sci. 44, 317–328.
Allen, D., 1971. The prediction sum of squares as a criterion for selection of predictor variables. University of Kentucky, Department of Statistics, Tech. Report 23.
Anderson, M.C., Neale, C.M.U., Li, F., Norman, J.M., Kustas, W.P., Jayanthi, H., Chavez, J., 2004. Upscaling ground observations of vegetation water content, canopy height, and leaf area index during SMEX02 using aircraft and Landsat imagery. Remote Sens. Environ. 92, 447–464.
Barilotti, A., Turco, S., Napolitano, R., Bressan, E., 2005. La tecnologia LiDAR per lo studio della biomassa negli ecosistemi forestali. In: 15th Meeting of the Italian Society of Ecology, Torino, Italy.
Bater, C.W., Wulder, M.A., Coops, N.C., Nelson, R.F., Hilker, T., Naesset, E., 2011. Stability of sample-based scanning-LiDAR-derived vegetation metrics for forest monitoring. IEEE Trans. Geosci. Remote Sens. 49, 2385–2392.
Belsley, D.A., 1984. Demeaning conditioning diagnostics through centering (with discussion). Am. Stat. 38, 73–77.
Birky, A.K., 2001. NDVI and a simple model of deciduous forest seasonal dynamics. Ecol. Model. 143, 43–58.
Bortolot, Z.J., Wynne, R.H., 2005. Estimating forest biomass using small footprint LiDAR data: an individual tree-based approach that incorporates training data. ISPRS J. Photogramm. Remote Sens. 59, 342–360.
Cannell, M.G.R., 1989. Physiological basis of wood production: a review. Scand. J. For. Res. 4, 459–475.
Carlson, C.A., Fox, T.R., Creighton, J., Dougherty, P.M., Johnson, J.R., 2009. Nine-year growth responses to planting density manipulation and repeated early fertilization in a loblolly pine stand in the Virginia Piedmont. South. J. Appl. For. 33, 109–114.
Carlyle, J.C., 1998. Relationships between nitrogen uptake, leaf area, water status and growth in an 11-year-old *Pinus radiata* plantation in response to thinning, thinning residue, and nitrogen fertiliser. For. Ecol. Manage. 108, 41–55.
Curran, P.J., Dungan, J.L., Gholz, H.L., 1992. Seasonal LAI in slash pine estimated with Landsat TM. Remote Sens. Environ. 39, 3–13.
Dalla-Tea, F., Jokela, E.J., 1991. Needlefall, canopy light interception, and productivity of young intensively managed slash and loblolly pine stands. For. Sci. 37, 1298–1313.
Dewey, J.C., Roberts, S.D., Hartley, I., 2006. A comparison of tools for remotely estimating leaf area index in loblolly pine plantations. In: Proceedings of the 13th Biennial Southern Silvicultural Research Conference. U.S. Department of Agriculture, Forest Service, Southern Research Station, Asheville, NC, pp. 71–75.
Drake, J.B., Knox, R.G., Dubayah, R.O., Clark, D.B., Condit, R., Blair, B.J., Hofton, M.A., 2003. Above-ground biomass estimation in closed canopy neotropical forests using lidar remote sensing: factors affecting the generality of relationships. Global Ecol. Biogeogr. 12, 147–159.

Eriksson, H.M., Eklundh, L., Kuusk, A., Nilson, T., 2006. Impact of understory vegetation on forest canopy reflectance and remotely sensed LAI estimates. Remote Sens. Environ. 103, 408–418.
Farid, A., Rautenkranz, D., Goodrich, D.C., Marsh, S.E., Sorooshian, S., 2006. Riparian vegetation classification from airborne laser scanning data with an emphasis on cottonwood trees. Can. J. Remote Sens. 32, 15–18.
Flores, F.J., Allen, H.L., Cheshire, H.M., Davis, J.G., Fuentes, M., Kelting, D.L., 2006. Using multispectral satellite imagery to estimate leaf area and response to silvicultural treatments in loblolly pine stands. Can. J. For. Res. 36, 1587–1596.
FPC, 2011. Forest Productivity Cooperative. Shaping the Future of Plantation Forestry, Raleigh, NC. <http://www.forestnutrition.org/> (August 2009).
Gholz, H.L., Curran, P.J., Kupiec, J.A., Smith, G.M., 1997. Assessing leaf area and canopy biochemistry of Florida pine plantations using remote sensing. In: Gholz, H.L., Nakane, K., Shimoda, H. (Eds.), The Use of Remote Sensing in the Modeling of Forest Productivity. Kluwer Academic Publishers, Dordrecht, The Netherlands.
Gresham, C.A., 1982. Litterfall patterns in mature loblolly and longleaf pine stands in coastal South Carolina. For. Sci. 28, 223–231.
Hebert, M.T., Jack, S.B., 1998. Leaf area index and site water balance of loblolly pine (*Pinus taeda* L.) across a precipitation gradient in east Texas. For. Ecol. Manag. 105, 273–282.
Hocking, R., 1976. The analysis and selection of variables in linear regression. Biometrics 32, 1–49.
Holmgren, J., 2004. Prediction of tree height, basal area and stem volume in forest stands using airborne laser scanning. Scand. J. For. Res. 19, 543–553.
Jensen, J.L.R., Humes, K.S., Vierling, L.A., Hudak, A.T., 2008. Discrete return lidar-based prediction of leaf area index in two conifer forests. Remote Sens. Environ. 112, 3947–3957.
Jensen, R.R., Binford, M.W., 2004. Measurement and comparison of leaf area index estimators derived from satellite remote sensing techniques. Int. J. Remote Sens. 25, 4251–4265.
Kwak, D.-A., Lee, W.-K., Cho, H.-K., 2007. Estimation of LAI using lidar remote sensing in forest. In: ISPRS Workshop on Laser Scanning and SilviLaser, Espoo, Finland, pp. 248–252.
Lefsky, M.A., Cohen, W.B., Harding, D.J., Parker, G.C., Acker, S.A., Gower, S.T., 2002a. Lidar remote sensing of above-ground biomass in three biomes. Global Ecol. Biogeogr. 11, 393–399.
Lefsky, M.A., Cohen, W.B., Parker, G.G., Harding, D.J., 2002b. Lidar remote sensing for ecosystem studies. Bioscience 52, 19–30.
LI-COR, 2010. FV2000 the LAI-2000 data file viewer. In: LI-COR Biosciences, Lincoln, NE, USA, p. 73.
Lovell, J.L., Jupp, D.L.B., Culvenor, D.S., Coops, N.C., 2003. Using airborne and ground-based ranging lidar to measure canopy structure in Australian forests. In: Workshop on 3-D Analysis of Forest Structure and Terrain Using LiDAR Technology. Canadian Aeronautics Space Inst., Victoria, Canada, pp. 607–622.
Lu, D., 2006. The potential and challenge of remote sensing-based biomass estimation. Int. J. Remote Sens. 27, 1297–1328.
Lutz, D.A., Washington-Allen, R.A., Shugart, H.H., 2008. Remote sensing of boreal forest biophysical and inventory parameters: a review. Can. J. For. Res. 34, S286–S313.
Magnussen, S., Boudewyn, P., 1998. Derivations of stand heights from airborne laser scanner data with canopy-based quantile estimators. Can. J. For. Res. 28, 1016–1031.
Maltamo, M., Eerikäinen, K., Pitkänen, J., Hyyppä, J., Vehmas, M., 2004. Estimation of timber volume and stem density based on scanning laser altimetry and expected tree size distribution functions. Remote Sens. Environ. 90, 319–330.
Marquart, D.W., 1980. Comment: you should standardize the predictor variables in your regression models. J. Am. Stat. Assoc. 75, 87–91.
Martin, T.A., Jokela, E.J., 2004. Developmental patterns and nutrition impact radiation use efficiency components in southern pine stands. Ecol. Appl. 14, 1839–1854.
McCombs, J.W., Roberts, S.D., Evans, D.L., 2003. Influence of fusing lidar and multispectral imagery on remotely sensed estimates of stand density and mean tree height in a managed loblolly pine plantation. For. Sci. 49, 457–466.
Morsdorf, F., Kötz, B., Meier, E., Itten, K.I., Allgöwer, B., 2006. Estimation of LAI and fractional cover from small footprint airborne laser scanning data based on gap fraction. Remote Sens. Environ. 104, 50–61.
Næsset, E., 1997a. Determination of mean tree height of forest stands using airborne laser scanner data. ISPRS J. Photogramm. Remote Sens. 52, 49–56.
Næsset, E., 1997b. Estimating timber volume of forest stands using airborne laser scanner data. Remote Sens. Environ. 61, 246–253.
Næsset, E., 2002. Predicting forest stand characteristics with airborne scanning laser using a practical two-stage procedure and field data. Remote Sens. Environ. 80, 88–99.
Nelson, R., Krabill, W., MacLean, G., 1984. Determining forest canopy characteristics using airborne laser data. Remote Sens. Environ. 15, 201–212.
Nelson, R., Oderwald, R., Gregoire, T.G., 1997. Separating the ground and airborne laser sampling phases to estimate tropical forest basal area, volume, and biomass. Remote Sens. Environ. 60, 311–326.
Nilsson, M., 1996. Estimation of tree heights and stand volume using an airborne lidar system. Remote Sens. Environ. 56, 1–7.
Ørka, H.O., Næsset, E., Bollandsås, O.M., 2009. Classifying species of individual trees by intensity and structure features derived from airborne laser scanner data. Remote Sens. Environ. 113, 1163–1174.
Peduzzi, A., Allen, H.L., Wynne, R.H., 2010. Leaf area of overstory and understory in pine plantations in the flatwoods. South. J. Appl. For. 34, 154–160.
Popescu, S.C., Wynne, R.H., Nelson, R., 2002. Estimating plot-level tree heights with lidar: local filtering with a canopy-height based variable window size. Comput. Electron. Agric. 37, 71–95.
Popescu, S.C., Wynne, R.H., Nelson, R.F., 2003. Measuring individual tree crown diameter with lidar and assessing its influence on estimating forest volume and biomass. Can. J. Remote Sens. 29, 564–577.
Rawlings, J.O., Pantula, S.G., Dickey, D.A., 2001. Applied Regression Analysis: A Research Tool, second ed. Springer, Ann Arbor, Michigan.
Riaño, D., Valladares, F., Condes, S., Chuvieco, E., 2004. Estimation of leaf area index and covered ground from airborne laser scanner (lidar) in two contrasting forests. Agric. For. Meteorol. 124, 269–275.
Roberts, S.D., Dean, T.J., Evans, D.L., McCombs, J.W., Harrington, R.L., Glass, P.A., 2005. Estimating individual tree leaf area in loblolly pine plantations using LiDAR-derived measurements of height and crown dimensions. For. Ecol. Manage. 213, 54–70.
Sampson, D.A., Albaugh, T.J., Johnsen, K.H., Allen, H.L., Zarnoch, S.J., 2003. Monthly leaf area index estimates from point-in-time measurements and needle phenology for *Pinus taeda*. Can. J. For. Res. 33, 2477–2490.
Sampson, D.A., Allen, H.L., 1995. Direct and indirect estimates of leaf-area index (lai) for lodgepole and loblolly-pine stands. Trees-Struct. Funct. 9, 119–122.
SAS, 2010. The SAS System for Windows Release 9.1.3. SAS Institute Inc., Cary, NC, USA.
Sasaki, T., Imanishi, J., Ioki, K., Morimoto, Y., Kitada, K., 2008. Estimation of leaf area index and canopy openness in broad leaved forest using an airborne laser scanner in comparison with high-resolution near-infrared digital photography. Landscape Ecol. Eng. 4, 47–55.
Schwarz, G., 1978. Estimating the dimension of a model. Ann. Stat. 6, 461–464.
Soudani, K., Trautmann, J., Walter, J.M.N., 2002. Leaf area index and canopy stratification in scots pine (*Pinus sylvestris* L.) stands. Int. J. Remote Sens. 23, 3605–3618.
Spanner, M.A., Pierce, L.L., Peterson, D.L., Running, S.W., 1990a. Remote-sensing of temperate coniferous forest leaf-area index – the influence of canopy closure, understory vegetation and background reflectance. Int. J. Remote Sens. 11, 95–111.
Spanner, M.A., Pierce, L.L., Running, S.W., Peterson, D.L., 1990b. The seasonality of AVHRR data of temperate coniferous forests: relationship with leaf area index. Remote Sens. Environ. 33, 97–112.
Turner, D.P., Cohen, W.B., Kennedy, R.E., Fassnacht, K.S., Briggs, J.M., 1999. Relationships between leaf area index and Landsat TM spectral vegetation indices across three temperate zone sites. Remote Sens. Environ. 70, 52–68.
van Aardt, J., Wynne, R.H., Oderwald, R.G., 2006. Forest volume and biomass estimation using small-footprint lidar-distributional parameters on a per-segment basis. For. Sci. 52, 636–649.
Vitousek, P.M., Matson, P.A., 1985. Disturbance, nitrogen availability, and nitrogen losses in an intensively managed loblolly-pine plantation. Ecology 66, 1360–1376.
Vose, J.M., Allen, H.L., 1988. Leaf area, stemwood growth, and nutrition relationships in loblolly pine. For. Sci. 34, 547–563.
Watson, D.J., 1947. Comparative physiological studies in the growth of field crops. I. Variation in net assimilation rate and leaf area between species and varieties, and within and between years. Ann. Bot-London 11, 41–76.
Welles, J.M., Norman, J.M., 1991. Instrument for indirect measurement of canopy architecture. Agron. J. 83, 818–825.
Zhao, K., Popescu, S., 2009. Lidar-based mapping of leaf area index and its use for validating GLOBCARBON satellite LAI product in a temperate forest of the southern USA. Remote Sens. Environ. 113, 1628–1645.